On-chip optical true time delay lines based on subwavelength grating waveguides

YUE WANG[1,2], HAO SUN[2], MOSTAFA KHALIL[2], WEI DONG[1], IVANA GASULLA[3], JOSÉ CAPMANY[3], AND LAWRENCE R. CHEN[2,*]

[1]*State Key Laboratory on Integrated Optoelectronics, College of Electronic Science and Engineering, Jilin University, Changchun 130012, China*
[2] *Department of Electrical and Computer Engineering, McGill University, Montreal, QC H3A 0E9, Canada*
[3] *ITEAM Research Institute, Universitat Politècnica de València, Valencia 46022, Spain*
**Corresponding author: lawrence.chen@mcgill.ca*

Received XX Month XXXX; revised XX Month, XXXX; accepted XX Month XXXX; posted XX Month XXXX (Doc. ID XXXXX); published XX Month XXXX

An optical true time delay line (OTTDL) is a fundamental building block for signal processing applications in microwave photonics (MWP) and optical communications. Here, we experimentally demonstrate an index-variable OTTDL based on an array of forty subwavelength grating (SWG) waveguides on silicon-on-insulator (SOI). Each SWG waveguide in the array is 34 mm long and arranged in a serpentine manner; the average incremental delay between waveguides is about 4.7 ps and the total delay between the first and last waveguides is approximately 181.9 ps. The waveguide array occupies a chip area of ~ 6.5 mm × 8.7 mm = 56.55 mm^2. The proposed OTTDLs bring potential advantages in terms of compactness as well as operation versatility to a variety of microwave signal processing applications.

http://dx.doi.org/10.1364/OL.99.099999

Microwave photonics (MWP) is an interdisciplinary area that combines microwave and optical engineering and focuses on the use of photonic means to generate, distribute, and process microwave signals [1]. The strong interest in MWP lies in its numerous intrinsic advantages, such as broad operation bandwidth, strong immunity to electromagnetic interference, and no limitation due to the electronic bottleneck effect [2]. Recently, considerable progress has been directed on developing photonic technologies to realize MWP signal processing functions [3]. One such technology is an optical true time delay line (OTTDL), which is a fundamental building block for MWP discrete-time signal processing applications [4]. For instance, they can be applied to reconfigurable MWP filters, arbitrary waveform generation/shaping, multi-cavity optoelectronic oscillation, and optical beamforming in phased array antennas [5]. Various approaches exist to implement OTTDLs in both fiber and integrated platforms, including switched variable-length waveguides [6], exploitation of the optical wavelength diversity through passive dispersive elements, e.g., chirped waveguide Bragg gratings [7], or exploiting the dispersion associated with a gain resonance, e.g., from stimulated Brillouin scattering [8]. Characteristics of OTTDLs include large delay, high resolution for continuously tunable delay or well defined delay steps for discretely tunable delays, broad operating bandwidth, and low loss. It is not necessary for an OTTDL to possess all these features simultaneously as the requirements will depend on the specific application.

There are two general approaches for implementing an optical delay line (ODL) [9]: (1) varying the propagation group velocity (v_g) (i.e., a wavelength-variable delay line) [10] and (2) varying the propagation length (L) of the delay element (i.e., a length-variable delay line) [6]. The wavelength-variable delay line will require different optical wavelengths to experience different propagation velocities and obtain different time delays. Thus, it cannot be used in the applications that require a time delay at the same wavelength. The length-variable delay line requires different lengths to obtain the different time delays, often resulting in a larger footprint or increased loss. An ODL providing time delays for pulses/signals having the same optical carrier is one form of an OTTDL.

Recently, there has been significant interest in developing subwavelength grating (SWG) waveguide structures for high-performance photonic integrated circuits in silicon-on-insulator (SOI) [11]. An SWG waveguide comprises a periodic arrangement of two different materials, one with a refractive index that is higher than the other, with a period (denoted Λ) that is small enough to suppress the diffraction effects. The characteristics of SWG waveguides, such as low loss and the flexibility to tailor the effective refractive index (through control of the duty cycle D, defined as the ratio between the length of the high refractive index material, denoted by a to the period, i.e., $D = a/\Lambda$), can result in enhanced performance compared to conventional SOI nanowire waveguide-based devices [12]. Gasulla and Capmany exploited the parallelism of multicore fibers (MCFs) and proposed their use as a sampled index-variable OTTDL for MWP applications [13]. Propagation of different groups delays over the same MCF was achieved by

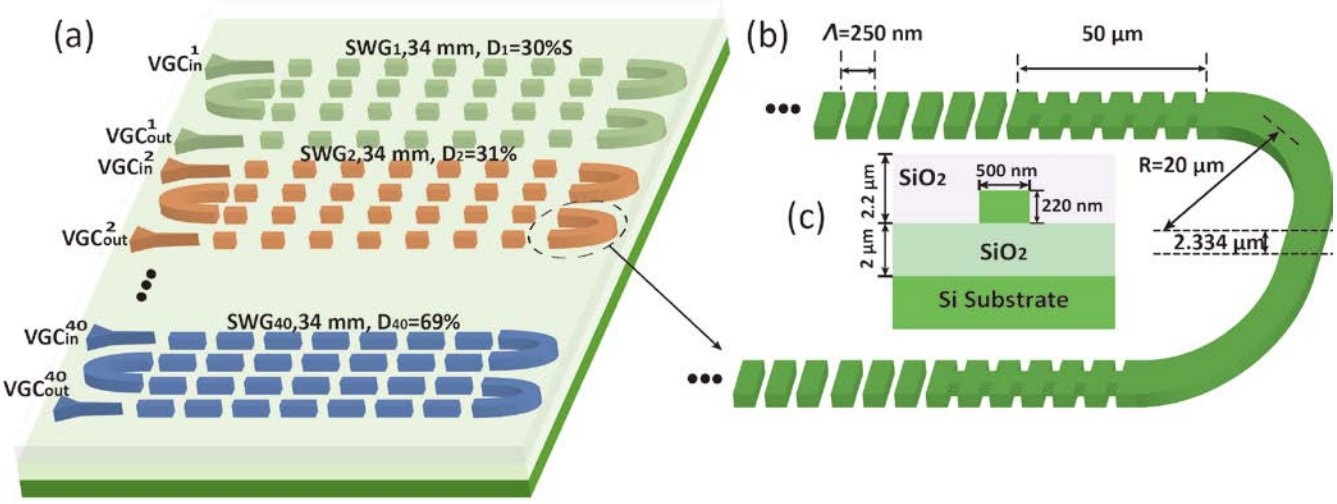

Fig. 1. Design of the SWG-waveguide-based OTTDL. (a) Schematic of the fabricated array of forty SWG waveguides in SOI (the different colors represent different duty cycles of the SWG waveguides). (b) Details of the waveguide bends. (c) The waveguide cross-section view.

properly designing the physical dimensions and material doping concentration of each core in a way that the cores feature the required differential chromatic dispersion profile for tunable operation [14]. Inspired by this approach, we proposed and demonstrated for the first time how a group of equal-length SWG waveguides can be used to implement an integrated version of a heterogeneous multicore fiber as a sampled index-variable OTTDL [15]. In particular, we showed that a group of four SWG waveguides of the same length can provide different propagation velocities by tailoring the effective index of each SWG waveguide through control of their corresponding duty cycles and verified its OTTDL nature.

Here, we significantly extend our proof-of-concept in [15] by making the following changes/advances: (1) we increase the length of the waveguides by more than a factor of 4 to 34 mm, (2) we use a serpentine arrangement, (3) we vary the duty cycle in 1% increments (as opposed to 10% increments), and (4) we realized forty SWG waveguides to provide 40 unique delay lines. These advances are significant because of the following: previously, we achieved a maximum differential delay (between the first and last waveguides) of only 27.5 ps with an average incremental delay (between consecutive waveguides) of 9.2 ps; on the other hand, we now achieve a maximum differential delay of 181.9 ps with an average incremental delay of only 4.7 ps. In other words, increasing the length of the waveguides allows for a greater maximum differential delay while reducing the duty cycles allows for a smaller incremental delay (it should be noted that smaller incremental delays are possible with shorter length waveguides). Moreover, the use of a serpentine arrangement for the longer waveguides has allowed us to maintain a similar chip length (i.e., 8.7 mm compared to 8.06 mm). Finally, with our new realization, we have been able to ascertain that a variation in duty cycle as low as 1% is possible and within fabrication capabilities. We also note that increasing the number of waveguides to 40 provides greater tunability/reconfigurability for systems applications, e.g., in microwave photonic filtering or optical beamforming, as well as flexibility, e.g., it is possible to use the same waveguide array to implement in parallel different signal processing functions, for instance, by devoting n samples (waveguides) to one functionality and the remaining 40-n samples to a second functionality.

An index-variable OTTDL generally involves waveguides of the same length but the propagation velocities are different. The group index of the SWG waveguides can be engineered to control the incremental time delay by choosing the duty cycles of each SWG

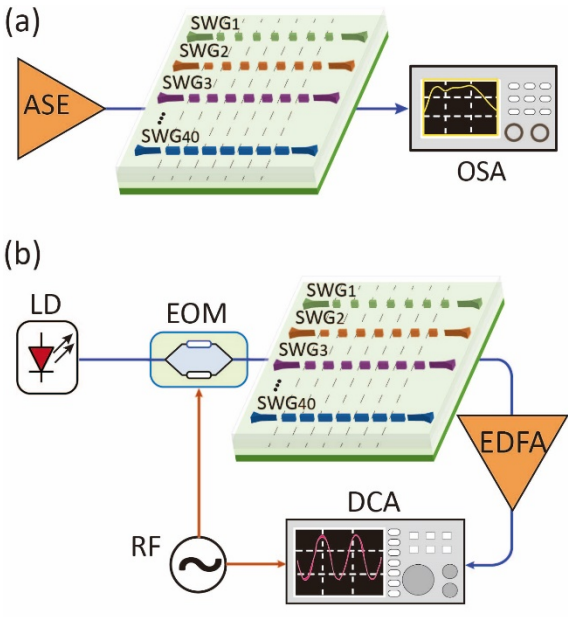

Fig. 2. (a) Experimental setup to measure the power spectral response of the fabricated index-variable OTTDL. (b) Experimental time-of-flight measurement setup. ASE: amplified spontaneous emission source; OSA: optical spectrum analyzer; LD: laser diode; EOM: electro-optic intensity modulator; EDFA: erbium-doped optical fiber amplifier; DCA: digital communication analyzer; RF: RF generator.

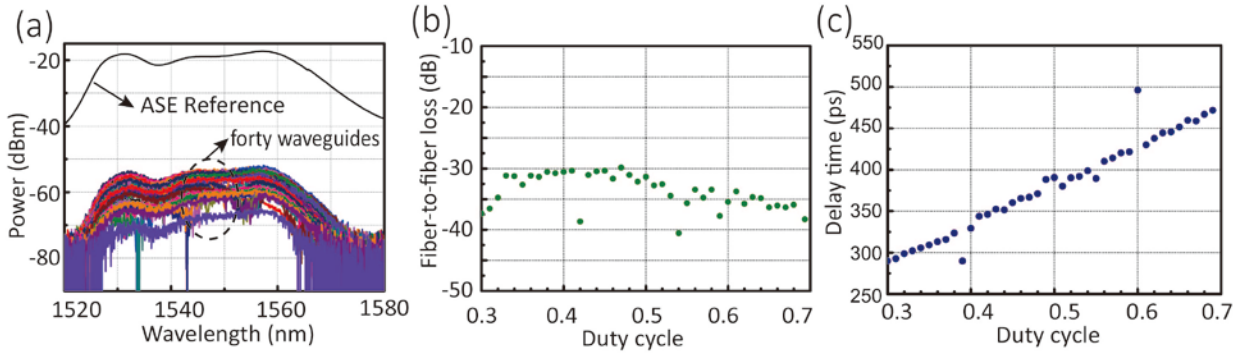

Fig. 3. (a) Measured power spectral responses based on ASE source. (b) Measured fiber-to-fiber loss of each SWG-based OTTDL. (c) Measured time delay of each OTTDL as a function the SWG duty cycle.

waveguides. The group index of an SWG waveguide can be expressed as [15]:

$$n_g = \frac{n_1 n_{g1} D + n_2 n_{g2}(1-D)}{\sqrt{D{n_1}^2 + (1-D){n_2}^2}}, \quad \textbf{(1)}$$

where n_1 and n_2 are the effective indices of the silicon and silica waveguides, respectively, n_{g1} and n_{g2} are the group index of the silicon and silica waveguides and D is the duty cycle of the SWG defined earlier.

To investigate the performance of the integrated index-variable OTTDL, we fabricated an array of forty SWG waveguides in SOI, see Fig. 1(a). The SWG waveguides are formed by alternating periodically segments of silicon and silica with a period of $\Lambda = 250$ nm. Each waveguide in the array is 34-mm long and the duty cycles are varied in 1% increments from 30% to 69%. The waveguides are arranged in a serpentine configuration to reduce size; each bend includes two SWG tapers to transition between the SWG waveguide and solid core waveguide used as the waveguide bend, as shown in Fig. 1(b). The SWG waveguides are separated by ~ 31.5 μm to eliminate crosstalk [16], which is small enough to ensure compactness. The array of waveguides occupies a total chip area of ~ 6.5 mm × 8.7 mm = 56.55 mm^2.

The chip is fabricated using electron beam lithography with a single etch at Applied Nanotools. The SWG waveguides have a cross-section of 220 nm × 500 nm; they are covered by an index-matched cladding layer of thickness 2.2 μm. Each SWG waveguide has an input and output taper for coupling to a nanowire waveguide of the same cross-section, as illustrated in Fig. 1(c). The SWG tapers are used for mode conversion between the SWG waveguide and the solid core waveguide [15]. The duty cycle of the taper is the same as the duty cycle of the SWG waveguide, and the thickness of waveguides is 220 nm. The length of a taper is 50 μm.

We use an EDFA as an amplified spontaneous emission (ASE) source and an optical spectrum analyzer (OSA) to obtain the spectral response of each SWG waveguide, as shown in Fig. 2(a). The experimental setup to measure the propagation time for the time-of-flight measurement is illustrated in Fig. 2(b). A tunable laser generates a continuous wave at 1550 nm with an output power of ~ 6 dBm. The laser is modulated employing an electro-optic modulator (EOM) driven by an RF signal of 10 GHz. After propagating through each SWG waveguide, the signals are amplified by a low-noise EDFA and then detected and observed using a digital communication analyzer (DCA). The incremental delays are extracted from the measured waveforms using the measured trace from the first waveguide as a reference.

Fig. 3(a) shows the spectra at the output of the waveguides as well as that of the input broadband source and confirms the broadband nature of the SWG waveguides (note that we did not optimize coupling for each measurement). To measure the total fiber-to-fiber loss, we replaced the ASE source by a laser set to 1550 nm and optimized the coupling for each SWG waveguide; the results are summarized in Fig. 3(b). The average fiber-to-fiber loss is approximately 33 dB, of which 20 – 22 dB is due to the vertical grating coupler (VGC) losses (measured separately using VGC-to-VGC test structures). Other losses include losses from the taper between nanowire and SWG waveguides, waveguide bend losses, and the propagation loss in the SWG waveguide. The taper losses between the nanowire and SWG waveguides vary with duty cycle and from simulations, we observe a loss of 0.07 - 0.08 dB/taper. We then estimate the total losses from the tapers to be 0.56 – 0.64 dB (there are 8 tapers in each waveguide). The loss of a nanowire waveguide bend with a bend radius > 10 μm is < 0.5 dB at 1550 nm [17]. The total losses from waveguide bends is then about 1.5 dB (there are 3 bends in each waveguide). Therefore, the SWG waveguide propagation losses are about 9 – 11 dB over their 34 mm length, corresponding to a propagation loss of 2.6 – 3.2 dB/cm, which agrees with values reported in the literature [18] as well as for conventional nanowire waveguides in SOI.

The total fiber-to-fiber loss can be reduced through the following. First, as the duty cycles of the SWG waveguides are varied, the corresponding tapers can be optimized separately to reduce the mode mismatch loss. Second, and most importantly, we can reduce the VGC coupling loss significantly: for instance, Wen *et al.* demonstrated a VGC design with a loss of 1.7 dB [19].

Through time-of-flight measurement, we get the results shown in Figs. 3(c) and 4. Fig. 3(c) shows the measured time delays in the waveguides, which increase linearly as a function of duty cycle (apart from a few waveguides which may have been impacted by fabrication and processing errors and variations given the small changes in duty cycle; we believe that these also contribute to the 'spikes' in the fiber-to-fiber losses shown in Fig. 3(b)). The average incremental time delay between consecutive SWG waveguides is about 4.7 ps. The total time delay between the first and last SWG waveguides is approximately 181.9 ps. Fig. 4 shows the measured time delays of the OTTDLs at different wavelengths. These results also verify that our index-variable OTTDL has a wide optical

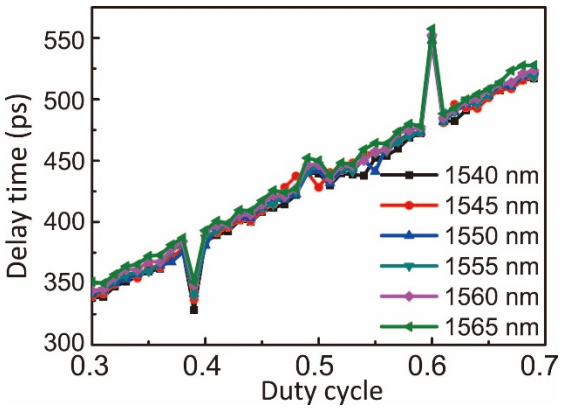

Fig. 4. Measured time delays of the 40 SWG waveguides at different wavelengths.

bandwidth from 1540 nm to 1565 nm (such a wide operating bandwidth can be useful in MWP applications requiring multiple optical carriers).

There are some advantages of our index-variable OTTDL comparing with other OTTDL approaches. For example, in the length-variable OTTDL in SOI in [20], obtaining a total delay of 180 ps requires a length difference of ~ 14 mm between the shortest and longest waveguides which will increase the size of the device. On the other hand, our index-variable OTTDL ensures that all SWG waveguides are of the same length. Another popular approach to implement ODLs is to use linearly chirped waveguide Bragg gratings [21]; however, as wavelength-variable ODLs, they cannot provide time delays for signals at the same wavelength. Moreover, obtaining a larger delay range requires longer waveguides. Finally, the use of coupled ring resonators requires careful control over the coupling coefficients [22]. Note that since the propagation losses in our SWG waveguides is comparable to those of nanowire waveguides in SOI, the loss per unit time delay is expected to be similar. Other material platforms, e.g., silicon nitride, offer lower propagation losses and potentially, lower loss per unit time delay.

We also note that continuous tuning of the delay should be possible by changing the wavelength of the optical carrier as observed using heterogeneous multicore fibers [14]. In particular, by operating closer to the SWG waveguide band edge, we may be able to take advantage of the increased dispersion in order to have different incremental values of dispersion and hence group delays as the wavelength of the optical carrier is tuned. In addition, increasing the number of SWG waveguides can provide more options for microwave photonics applications. It should be possible to increase the number of the SWG waveguides by reducing the increment in duty cycle. For example, the increment in duty cycle can be reduced or the range of duty cycles can be increased, thereby allowing for an increase in the number of SWG waveguides in the array. However, these will be limited by either the resolution of ebeam lithography or higher taper and propagation losses [16, 23].

In summary, we have proposed and designed experimentally an OTTDL based on an array of forty SWG waveguides in SOI, where each waveguide is 34-mm long. By controlling the duty cycles which are varied in 1% increments from 30% to 69%, an average incremental delay of about 4.7 ps and a total delay between the first and last waveguides of approximately 181.9 ps can be obtained. Our work has allowed us to achieve a higher performance OTTDL while ensuring a compact size, enhance applications with one single chip, and allow us to establish what can be realized with existing fabrication capabilities. We believe that our SWG-waveguide-based OTTDL offers a versatile and compact solution to enable a wide range of integrated MWP signal processing functions for enhanced radar, communications, sensing, and instrumentation applications. Beyond MWP, this approach can be extended to perform additional optical signal processing applications that require different values of the group delay.

Funding. Natural Sciences and Engineering Research Council of Canada; China Scholarship Council; European Research Council under Consolidator Grant Project (724663).

References

1. J. Capmany, J. Mora, I. Gasulla, J. Sancho, J. Lloret, and S. Sales, J. Light. Technol. **31**, 571 (2012).
2. J. Capmany, and D. Novak, Nat. Photonics **1**, 319 (2007).
3. C. G. H. Roeloffzen, L. Zhuang, C. Taddei, A. Leinse, R. G. Heideman, P. W. L. Van Dijk, R. M. Oldenbeuving, D. A. I. Marpaung, M. Burla, and K. J. Boller, Opt. Express **21**, 22937-22961 (2013).
4. R. A. Minasian, E. H. W. Chan, and X. Yi, Opt. Express **21**, 22918 (2013).
5. J.-D. Shin, B.-S. Lee, and B.-G. Kim, IEEE Photon. Technol. Lett. **16**, 1364-1366 (2004).
6. X. Ye, F. Zhang, and S. Pan, Opt. Express **23**, 10002 (2015).
7. I. Giuntoni, D. Stolarek, D. I. Kroushkov, J. Bruns, L. Zimmermann, B. Tillack, and K. Petermann, Opt. Express **20**, 11241 (2012).
8. A. Choudhary, Y. Liu, B. Morrison, K. Vu, D. Y. Choi, P. Ma, S. Madden, D. Marpaung, and B. J. Eggleton, Sci. Rep. **7**, 5932 (2017).
9. L. R. Chen, J. Light. Technol. **35**, 824 (2016).
10. J. Xie, L. Zhou, Z. Zou, J. Wang, and J. Chen, Opt. Express **22**, 817 (2014).
11. P. Cheben, R. Halir, J. H. Schmid, H. A. Atwater, and D. R. Smith, Nature **560**, 565 (2018)..
12. P. J. Bock, P. Cheben, J. H. Schmid, J. Lapointe, A. Delâge, S. Janz, G. C. Aers, D.-X. Xu, A. Densmore, and T. J. Hall, Opt. Express **18**, 20251 (2010).
13. I. Gasulla, and J. Capmany, IEEE Photon. J. **4**, 877 (2012).
14. S. García, and I. Gasulla, Opt. Express **24**, 20641 (2016).
15. J. Wang, R. Ashrafi, R. Adams, I. Glesk, I. Gasulla, J. Capmany, and L. R. Chen, Sci. Rep. **6**, 30235 (2016).
16. V. Donzella, A. Sherwali, J. Flueckiger, S. T. Fard, S. M. Grist, and L. Chrostowski, Opt. Express **22**, 21037 (2014).
17. L. Chrostowski, and M. Hochberg, *Silicon Photonics Design: From Devices to Systems* (2015).
18. L. R. Chen, J. Wang, B. Naghdi, and I. Glesk, "Subwavelength Grating Waveguide Devices for Telecommunications Applications," IEEE J. Sel. Top. Quantum Electron. **25**, 82001 (2018).
19. W. Zhou, Z. Cheng, X. Chen, K. Xu, X. Sun, and H. K. Tsang, IEEE J. Sel. Top. Quantum Electron. **25**, 2900113 (2019).
20. J. Xie, L. Zhou, Z. Li, J. Wang, and J. Chen, Opt. Express **22**, 22707 (2014).
21. W. Zhang and J. Yao, J. Light. Technol. **34**, 4664 (2016).
22. M. S. Rasras, C. K. Madsen, and M. A. Cappuzzo, IEEE Photon. Technol. Lett. **17**, 834 (2005).
23. L. Chrostowski, X. Wang, J. Flueckiger, Y. Wu, Y. Wang, and S. T. Fard, in *Optical Fiber Communication Conference*(Optical Society of America 2014), p. 37.

1. J. Capmany, J. Mora, I. Gasulla, J. Sancho, J. Lloret, and S. Sales, "Microwave photonic signal processing," J. Light. Technol. **31**, 571-586 (2012).
2. J. Capmany, and D. Novak, "Microwave photonics combines two worlds," Nat. Photonics **1**, 319-330 (2007).
3. C. G. H. Roeloffzen, L. Zhuang, C. Taddei, A. Leinse, R. G. Heideman, P. W. L. Van Dijk, R. M. Oldenbeuving, D. A. I. Marpaung, M. Burla, and K. J. Boller, "Silicon nitride microwave photonic circuits," Opt. Express **21**, 22937-22961 (2013).
4. R. A. Minasian, E. H. W. Chan, and X. Yi, "Microwave photonic signal processing," Opt. Express **21**, 22918-22936 (2013).
5. J.-D. Shin, B.-S. Lee, and B.-G. Kim, "Optical true time-delay feeder for X-band phased array antennas composed of 2/spl times/2 optical MEMS switches and fiber delay lines," IEEE Photon. Technol. Lett. **16**, 1364-1366 (2004).
6. X. Ye, F. Zhang, and S. Pan, "Optical true time delay unit for multi-beamforming," Opt. Express **23**, 10002-10008 (2015).
7. I. Giuntoni, D. Stolarek, D. I. Kroushkov, J. Bruns, L. Zimmermann, B. Tillack, and K. Petermann, "Continuously tunable delay line based on SOI tapered Bragg gratings," Opt. Express **20**, 11241-11246 (2012).
8. A. Choudhary, Y. Liu, B. Morrison, K. Vu, D. Y. Choi, P. Ma, S. Madden, D. Marpaung, and B. J. Eggleton, "High-resolution, on-chip RF photonic signal processor using Brillouin gain shaping and RF interference," Sci. Rep. **7**, 5932 (2017).
9. L. R. Chen, "Silicon photonics for microwave photonics applications," J. Light. Technol. **35**, 824-835 (2016).
10. J. Xie, L. Zhou, Z. Zou, J. Wang, and J. Chen, "Continuously tunable reflective-type optical delay lines using microring resonators," Opt. Express **22**, 817-823 (2014).
11. P. Cheben, R. Halir, J. H. Schmid, H. A. Atwater, and D. R. Smith, "Subwavelength integrated photonics," Nature **560**, 565-572 (2018).
12. P. J. Bock, P. Cheben, J. H. Schmid, J. Lapointe, A. Delâge, S. Janz, G. C. Aers, D.-X. Xu, A. Densmore, and T. J. Hall, "Subwavelength grating periodic structures in silicon-on-insulator: a new type of microphotonic waveguide," Opt. Express **18**, 20251-20262 (2010).
13. I. Gasulla, and J. Capmany, "Microwave photonics applications of multicore fibers," IEEE Photon. J. **4**, 877-888 (2012).
14. S. García, and I. Gasulla, "Dispersion-engineered multicore fibers for distributed radiofrequency signal processing," Opt. Express **24**, 20641-20654 (2016).
15. J. Wang, R. Ashrafi, R. Adams, I. Glesk, I. Gasulla, J. Capmany, and L. R. Chen, "Subwavelength grating enabled on-chip ultra-compact optical true time delay line," Sci. Rep. **6**, 30235 (2016).
16. V. Donzella, A. Sherwali, J. Flueckiger, S. T. Fard, S. M. Grist, and L. Chrostowski, "Sub-wavelength grating components for integrated optics applications on SOI chips," Opt. Express **22**, 21037-21050 (2014).
17. L. Chrostowski, and M. Hochberg, *Silicon Photonics Design: From Devices to Systems* (2015).
18. L. R. Chen, J. Wang, B. Naghdi, and I. Glesk, "Subwavelength grating waveguide devices for telecommunications applications," IEEE J. Sel. Top. Quantum Electron., **25**, 82001 (2018).
19. W. Zhou, Z. Cheng, X. Chen, K. Xu, X. Sun, and H. K. Tsang, "Subwavelength engineering in silicon photonic devices," IEEE J. Sel. Top. Quantum Electron. **25**, 2900113 (2019).
20. J. Xie, L. Zhou, Z. Li, J. Wang, and J. Chen, "Seven-bit reconfigurable optical true time delay line based on silicon integration," Opt. Express **22**, 22707-22715 (2014).
21. W. Zhang, and J. Ya, "Silicon-based on-chip electrically-tunable spectral shaper for continuously tunable linearly chirped microwave waveform generation," J. Light. Technol. **34**, 4664-4672 (2016).
22. M. S. Rasras, C. K. Madsen, and M. A. Cappuzzo, "Integrated resonance-enhanced variable optical delay lines," IEEE Photon. Technol. Lett. **17**, 834-836 (2005).
23. L. Chrostowski, X. Wang, J. Flueckiger, Y. Wu, Y. Wang, and S. T. Fard, "Impact of fabrication non-uniformity on chip-scale silicon photonic integrated circuits," in *Optical Fiber Communication Conference*(Optical Society of America2014), p. Th2A. 37.